

Cable theory of protein receptor trafficking in a dendritic tree

Paul C. Bressloff

*Department of Mathematics, University of Utah, Salt Lake City, Utah 84112, USA
and Mathematical Institute, University of Oxford, 24-29 St. Giles', Oxford OX1 3LB, United Kingdom*

(Received 7 November 2008; published 3 April 2009)

We develop an application of linear cable theory to protein receptor trafficking in the surface membrane of a neuron's dendritic tree. We assume that receptors diffuse freely in the dendritic membrane but exhibit periods of confined motion through interactions with small mushroomlike protrusions known as dendritic spines. We use cable theory to determine how receptor trafficking depends on the geometry of the dendritic tree and various important biophysical parameters such as membrane diffusivity, the density of spines, the strength of diffusive coupling between dendrites and spines, and the rates of constitutive recycling of receptors between the surface of spines and intracellular pools. We also use homogenization theory to determine corrections to cable theory arising from the discrete nature of spines.

DOI: [10.1103/PhysRevE.79.041904](https://doi.org/10.1103/PhysRevE.79.041904)

PACS number(s): 87.16.A-, 87.19.L-, 87.10.-e

I. INTRODUCTION

Recent fluorescent recovery after photobleaching and single-particle tracking experiments have revealed that neurotransmitter receptors undergo periods of free diffusion within the dendritic membrane of a neuron interspersed with periods of restricted motion in confinement domains that coincide with synapses [1–6]. Most excitatory synapses in the brain are located within dendritic spines, which are small, submicrometer membranous extrusions that protrude from a dendrite. Typically spines have a bulbous head which is connected to the parent dendrite through a thin spine neck. Confinement of receptors occurs due to the geometry of the spine and through interactions with scaffolding proteins and cytoskeletal elements within the postsynaptic density (PSD), which is the protein-rich region at the tip of the spine head. Moreover, receptors within a spine may be internalized by endocytosis and then either reinserted into the surface membrane via exocytosis or degraded [7]. It follows that under basal conditions, the steady-state receptor concentration within a synapse is determined by a dynamical equilibrium in which the various receptor fluxes into and out of the spine are balanced. Activity-dependent changes in one or more of these fluxes can then modify the number of receptors in the spine and thus alter the strength or weight of a synapse. This is particularly significant, since there is now a large body of experimental evidence suggesting that the activity-dependent regulation of the trafficking of α -amino-3-hydroxy-5-methyl-4-isoxazole-propionic acid (AMPA) receptors, which mediate the majority of fast excitatory synaptic transmission in the central nervous system, plays an important role in synaptic plasticity [8–10].

In a previous paper [11], we analyzed a two-dimensional diffusion model of protein receptor trafficking on a cylindrical dendritic membrane containing a population of dendritic spines, which acted as spatially localized traps. We treated the transverse intersection of a spine and a dendrite as a small, partially absorbing boundary and used singular perturbation theory to analyze the steady-state distribution of receptors in the dendrite and spines. Using a combination of analysis and numerical simulations, we showed that under

normal physiological conditions the variation in receptor concentration around the circumference of the dendrite is negligible, thus justifying a reduction to a one-dimensional model. In the reduced model one can ignore the spatial extent of each spine and represent the density of spines along the dendrite as a discrete sum of Dirac delta functions [12]. This is motivated by the observation that the spine neck, which forms the junction between a synapse and its parent dendrite, varies in radius from ~ 0.02 to $0.2 \mu\text{m}$, which is typically an order of magnitude smaller than the spacing between spines (~ 0.1 – $1 \mu\text{m}$) and the circumference of the dendritic cable ($\sim 1 \mu\text{m}$); see Ref. [13]. In other words, the disklike region or hole forming the junction between a spine and the dendritic cable is relatively small, and can therefore be neglected in the one-dimensional model. In the full two-dimensional model of a dendritic cable, however, one can no longer treat the spines as pointlike objects due to the fact that the Green's function associated with two-dimensional diffusion has a logarithmic singularity [11].

More recently we have carried out a further simplification of the one-dimensional model by treating the spine density and biophysical properties of the spines as continuous functions of spatial position along the dendrite [14]. One of the major advantages of this continuum approximation is that we can adapt many methods and results from linear cable theory. The latter was originally developed by Rall in order to describe the large-scale electronic structure of dendritic trees (see the collection of papers in Ref. [15]), and has subsequently been used to analyze linearized reaction-diffusion equations describing the diffusion and buffering of calcium ions and other second messengers in the dendritic cytoplasm [16,17]. Cable theory has proven to be a very powerful tool for quantifying how dendritic structure influences the electrophysiological properties of a neuron, and has led to many new insights into the possible computational role of dendrites and spines [18].

In this paper, we present a major application of cable theory, namely, analyzing the role of surface diffusion and dendritic structure on the trafficking of neurotransmitter receptors across multiple synapses. In particular, we use cable theory to quantify how the distribution of receptors depends on the geometry of the tree and various important biophys-

cal parameters such as membrane diffusivity, the density of spines, the strength of diffusive coupling between dendrites and spines, and the rates of constitutive recycling of receptors between the surface of spines and intracellular pools. As we have illustrated elsewhere [14], the development of such a theory is important, since it provides a quantitative framework for interpreting biophysical experiments concerned with global aspects of receptor trafficking, such as inferring relaxation rates from surface-inactivation experiments. It also allows the construction of biophysical and computational models of synaptic plasticity that take into account diffusion-mediated changes in the number of synaptic receptors following chemical or electrical stimulation. Although our model and choice of parameters are mainly based on experimental data of AMPA receptor trafficking, the underlying theory is applicable to the more general problem of membrane diffusion and its role in protein receptor trafficking.

The structure of the paper is as follows. The continuum model is introduced in Sec. II and steady-state solutions are analyzed in Sec. III. We show that the steady-state equation is given by a linear cable equation, which allows us to identify an effective space constant for receptor diffusion and to derive an analog of the “equivalent-cylinders” representation of a branched dendritic cable [19,20]. That is, the steady-state solution can be obtained by reducing a branched cable to a single equivalent cable under the constraint that at each node the diameters d_1, d_2 of the two daughter branches are related to the diameter of the parent branch according to the rule $\sqrt{d} = \sqrt{d_1} + \sqrt{d_2}$. Such a constraint will not be satisfied by most dendritic geometries and the reduction cannot be extended to time-dependent solutions, so we consider a more general approach to handling branching structures in Sec. V. In Sec. IV we consider a discrete set of spines whose mean spacing is much smaller than the space constant of the corresponding continuum model so that there is a separation of spatial scales. We then use a multiscale homogenization procedure to analyze small-scale fluctuations in the steady-state receptor concentration, following along similar lines to a recent analysis of the cable equation for membrane voltage in a heterogeneous dendrite [21]. In particular, we show that the continuum approximation is reasonable provided that the diffusive coupling between spines and the parent dendrite is sufficiently weak. In Sec. V we use Laplace transforms to calculate the Green’s function for the full time-dependent model, which takes into account the internal receptor dynamics of spines. The Green’s function determines the time-dependent dendritic receptor concentration in response to both somatic and intracellular sources of receptors. We also perform an asymptotic analysis of the Green’s function in order to extract the asymptotic rate of relaxation to the steady state. Finally, we show how to construct the Green’s function on an arbitrary dendritic tree using the so-called sum-over-trips formalism developed originally by Abbott *et al.* [22] for electrically passive dendritic trees (see also Refs. [23,24]), and extended more recently to quasiactive dendrites by Coombes *et al.* [25].

II. CONTINUUM MODEL OF RECEPTOR TRAFFICKING

Consider a single uniform dendritic cable of length L and circumference l as shown in Fig. 1(a). Let $U(x, t)$, with

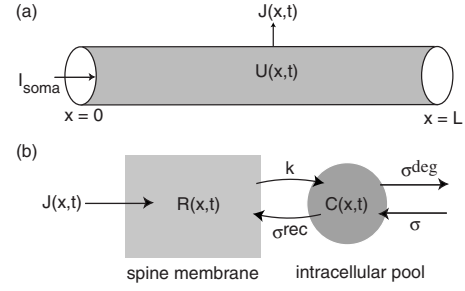


FIG. 1. Continuum model of protein receptor trafficking along a dendrite. (a) Single dendritic cable. The concentration $U(x, t)$ of surface receptors at time t varies with distance x from the soma. A surface receptor current I_{soma} is injected at the somatic end of the cable. The current $J(x, t)$ determines the rate at which receptors flow between the dendrite and an individual spine at x . (b) Simplified model of a spine showing constitutive recycling with an intracellular pool. Surface receptors of concentration $R(x, t)$ are internalized at a rate k and are either reinserted into the spine surface from an intracellular pool of $C(x, t)$ receptors at a rate σ^{rec} or sorted for degradation at a rate σ^{deg} . There is also a local production of intracellular receptors at a rate σ .

$0 \leq x \leq L$, denote the concentration of receptors within the surface of the dendrite at time t and position x , where x denotes axial distance from the soma. Following Ref. [14], we model the one-dimensional diffusive transport of surface receptors along the dendritic cable according to the equation

$$\frac{\partial U}{\partial t} = D \frac{\partial^2 U}{\partial x^2} - \rho(x)J(x, t). \quad (2.1)$$

The first term on the right-hand side of Eq. (2.1) represents the Brownian diffusion of receptors along the surface of the cable, whereas the second term represents the flux of receptors from the dendrite to a local population of dendritic spines, with $\rho(x)$ denoting the spine density and $J(x, t)$ representing the number of receptors per unit time flowing into a single spine at x . The density ρ satisfies the normalization condition $\int_0^L \rho(x) dx = N/l$, where N is the total number of spines on the dendrite. Equation (2.1) is supplemented by boundary conditions at the ends of the cable:

$$D \left. \frac{\partial U}{\partial x} \right|_{x=0} = -\frac{I_{\text{soma}}}{l}, \quad D \left. \frac{\partial U}{\partial x} \right|_{x=L} = 0. \quad (2.2)$$

Here I_{soma} represents a current source (number of surface receptors per unit time) at the boundary $x=0$ adjacent to the soma arising from fast somatic exocytosis [26]. The distal end of the cable at $x=L$ is taken to be closed.

Denoting the concentration of surface receptors in an individual spine at x by $R(x, t)$, we take the receptor current $J(x, t)$ to be of the form

$$J(x, t) = \Omega_+ U(x, t) - \Omega_- R(x, t), \quad (2.3)$$

where Ω_{\pm} are effective hopping rates into and out of the spine. In previous work [11,12], we have taken $\Omega_{\pm} = \Omega$, with Ω representing the effects of the spine neck on restricting the flow of receptors [4]. However, there are additional factors that confine receptors within a spine such as interactions with

scaffolding proteins and cytoskeletal elements. Such effects can be incorporated into our simplified single-spine model by taking the rate of exit from a spine to be smaller than the rate of entry; that is, $\Omega_- < \Omega_+$. Substitution of Eq. (2.3) into Eq. (2.1) then gives

$$\frac{\partial U}{\partial t} = D \frac{\partial^2 U}{\partial x^2} - \rho(x)[\Omega_+ U(x,t) - \Omega_- R(x,t)]. \quad (2.4)$$

The dynamics of the receptor concentration $R(x,t)$ within an individual spine is determined by the current across the junction with the dendritic cable, and the various forms of local trafficking within a spine. A detailed model of single-spine dynamics has been presented elsewhere [27,28]. Here we follow Refs. [11,12] and consider a simplified model in which we treat the spine as a single homogeneous compartment; see Fig. 1(b). We assume that surface receptors within a spine are endocytosed at a rate k and stored in a corresponding intracellular pool [7,29,30]. Intracellular receptors are either reinserted into the surface via exocytosis at a rate σ^{rec} or degraded at a rate σ^{deg} . Denoting the number of receptors in an intracellular pool at (x,t) by $C(x,t)$, we then have the pair of equations

$$A \frac{\partial R}{\partial t} = \Omega_+ U - \Omega_- R - kR + \sigma^{\text{rec}} C, \quad (2.5)$$

$$\frac{\partial C}{\partial t} = -\sigma^{\text{rec}} C - \sigma^{\text{deg}} C + kR + \sigma. \quad (2.6)$$

The first two terms on the right-hand side of Eq. (2.5) constitute the current $J(x,t)$ of Eq. (2.3). Since $J(x,t)$ is the *number* of receptors per unit time flowing across the junction between the dendritic cable and the spine, it is necessary to multiply the left-hand side by the surface area A of the spine in order to properly conserve receptor numbers. We also allow for a local source of intracellular receptors by including the inhomogeneous term σ on the right-hand side of Eq. (2.6). This represents the local accumulation of new (rather than recycled) receptors within the intracellular pool supplied, for example, by the targeted delivery of intracellular receptors from the soma [31,32], or possibly by local receptor synthesis [33–35]. Note that all parameters in Eqs. (2.4)–(2.6) could themselves be functions of x and t , although in this paper we will restrict ourselves to the case of identical spines with time-independent properties.

The model given by Eqs. (2.4)–(2.6) treats the surface of the dendritic cable as an effective one-dimensional medium, in which variations in the dendritic receptor concentration around the circumference of the cable are neglected. This can be justified by considering a reduction from a full two-dimensional model of surface diffusion in which the junction between each spine and the dendritic surface is treated as a small, partially absorbing trap [11,12]. Such a reduction leads to Eq. (2.4) with the spine density given by a sum of Dirac delta functions:

$$\rho(x) = \frac{1}{l} \sum_{j=1}^N \delta(x - x_j), \quad (2.7)$$

where x_j is the location of the j th spine. Following Ref. [14], we will make an additional simplification by taking the spine density ρ and the various biophysical parameters characterizing individual spines ($\Omega_{\pm}, k, \sigma^{\text{rec}}, \sigma^{\text{deg}}, \sigma$) to be continuous functions of x . We expect this continuum approximation to be reasonable in the case of a large number of closely spaced spines such that neighboring spines share similar properties (perhaps after spatially averaging over local clusters of spines). In Sec. IV we will show how corrections to this continuum approximation can be obtained using a multiple-scale homogenization procedure, following along similar lines to the recent analysis of voltage and conductance changes in a heterogeneous dendrite [21].

Although we focus on the dynamics of receptor trafficking in this paper, it is useful to explain briefly how our biophysical model can be incorporated into more physiological descriptions of synaptic function. Each excitatory synapse on the postsynaptic side can be identified with the PSD located within the spine head. Assuming a uniform concentration R of receptors in the spine, the total number of synaptic receptors is aR , where a is the area of the PSD. The arrival of an action potential at the presynaptic terminal leads to the release of chemical neurotransmitters, which bind to receptors within the PSD. This changes the configurational state of each receptor, resulting in the transient opening of an ion channel and the flow of ions through the cell membrane. Assuming that all synaptic receptors bind to neurotransmitter and have identical conductance states g_S , the total change in synaptic conductance is $g_S a R$. The maximal conductance change is one measure of the strength of a synapse. Of course, this is an oversimplification since there can be different classes of receptors and the conductance of a receptor may be modified by interactions with scaffolding proteins and other protein complexes within the PSD. Nevertheless, even in this simplified model, we see that the strength of a synapse depends on a number of factors including the concentration of receptors within a spine, the area of the PSD, and the conductance state of the receptors. All of these are potential targets for chemical signaling cascades that induce activity-dependent changes in the strength of a synapse. Since there is growing experimental evidence that changes in synaptic strength are associated with changes in the number of synaptic AMPA receptors [8–10], it follows that the cable theory of receptor trafficking also has applications to biophysical and computational models of synaptic plasticity; see Ref. [14].

III. STEADY-STATE CABLE EQUATION

In this section we calculate the steady-state receptor concentration U on a branched dendrite, in which each branch is treated as a uniform cable with identical uniformly distributed spines. Note that as one proceeds away from the soma, dendrites tend to become thinner. This is partially taken into account by taking daughter branches to be thinner than their parent branch. However, one could also extend the analysis

to the case of tapering dendrites, in which the diameter of a cable decreases smoothly with distance along the cable [36,37].

A. Single uniform cable

We begin by considering a single branch as shown in Fig. 1. In the case of a constant current I_{soma} at the end $x=0$, solutions of Eqs. (2.4)–(2.6) converge to a unique steady state obtained by setting all time derivatives to zero. Equations (2.5) and (2.6) imply that in the steady state

$$C(x) = \frac{kR(x) + \sigma}{\sigma^{\text{rec}} + \sigma^{\text{deg}}}, \quad R(x) = \frac{\Omega_+ U(x) + \Lambda \sigma}{\Omega_- + k(1 - \Lambda)}, \quad (3.1)$$

where

$$\Lambda = \frac{\sigma^{\text{rec}}}{\sigma^{\text{rec}} + \sigma^{\text{deg}}}.$$

Substituting Eq. (3.1) into the steady-state version of diffusion equation (2.4) gives

$$D \frac{d^2 U}{dx^2} - \rho(x) \bar{\Omega} [U(x) - \bar{R}] = 0, \quad (3.2)$$

where

$$\bar{\Omega} = \frac{\Omega_+ k(1 - \Lambda)}{\Omega_- + k(1 - \Lambda)}, \quad \bar{R} = \frac{\Omega_-}{\Omega_+} \frac{\Lambda \sigma}{k(1 - \Lambda)}. \quad (3.3)$$

One can view $\bar{\Omega}$ as an effective spine-neck hopping rate and \bar{R} as an effective spine receptor concentration. Equation (3.2) is supplemented by boundary conditions (2.2). Since the steady-state receptor concentration within spines, $R(x)$, is a simple monotonic function of the dendritic receptor concentration $U(x)$, we will focus on solutions of the latter.

In the case of a uniform spine density, $\rho(x) = \rho_0 = 1/l\Delta$, with $\Delta = L/N$ as the mean spacing between spines, Eq. (3.2) reduces to the simpler form [14]

$$\frac{d^2 U}{dx^2} - \gamma^2 U(x) = -\gamma^2 \bar{R}, \quad (3.4)$$

where

$$\gamma = \sqrt{\frac{\rho_0 \bar{\Omega}}{D}} = \sqrt{\frac{\bar{\Omega}}{l\Delta D}}. \quad (3.5)$$

Integrating Eq. (3.4) with respect to x and using boundary conditions (2.2) yields the conservation condition

$$I_{\text{soma}} = N \bar{\Omega} \left[\int_0^L U(x) dx / L - \bar{R} \right].$$

This implies that the total number of receptors entering the dendrite from the soma is equal to the mean number of receptors hopping from the dendrite into the N spines.

Equation (3.4) is identical in form to the steady-state cable equation describing membrane voltage and electrical current flow in passive dendrites [15,17,19,20] with $\gamma^{-1} \equiv \xi$ reinterpreted as an effective space constant for surface recep-

tor diffusion and transport. (The background term \bar{R} plays an analogous role to the membrane reversal potential in a dendrite that is uniformly stimulated by background synaptic currents with voltage-independent conductances.) The general solution of Eq. (3.4) is given by

$$U(x) = A \cosh(\gamma x) + B \sinh(\gamma x) + \bar{R}, \quad (3.6)$$

with the constants A, B determined by boundary conditions (2.2). In anticipation of our analysis of branching structures, we generalize these boundary conditions by introducing the notion of a diffusive impedance (borrowing terminology from corresponding studies of the linear cable equation for membrane voltage [17,38]). First, we define a diffusive receptor current $I(x)$ along the cable [as distinct from the diffusive current $J(x)$ between dendrite and spines] according to

$$I = -lD \frac{\partial U}{\partial x}. \quad (3.7)$$

It follows that the steady-state current is given by

$$I(x) = -Z^{-1} [A \sinh(\gamma x) + B \cosh(\gamma x)], \quad (3.8)$$

where

$$Z = \frac{1}{lD\gamma} = \sqrt{\frac{\Delta}{lD\bar{\Omega}}} \quad (3.9)$$

is the *characteristic diffusive impedance* of the cable. We then introduce a Robin boundary condition at the end $x=L$ so that

$$I(0) = I_{\text{soma}}, \quad U(L) - \bar{R} = Z_L I(L), \quad (3.10)$$

where Z_L is a *terminal diffusive impedance* due to a possible diffusive coupling with secondary branches at $x=L$ (see below). We recover the closed or Neumann boundary condition of Eq. (2.2) by taking the infinite-impedance limit $Z_L \rightarrow \infty$. On the other hand, the zero-impedance limit $Z_L \rightarrow 0$ corresponds to the Dirichlet boundary condition $U(L) = \bar{R}$.

A straightforward calculation shows that the steady-state receptor concentration for boundary conditions (3.10) is given by [38]

$$U(x) = Z I_{\text{soma}} \frac{Z \sinh(\gamma[L-x]) + Z_L \cosh(\gamma[L-x])}{Z \cosh(\gamma L) + Z_L \sinh(\gamma L)} + \bar{R}. \quad (3.11)$$

If the boundary at $x=L$ is also closed as in Eq. (2.2), then

$$U(x) = Z I_{\text{soma}} \frac{\cosh(\gamma[x-L])}{\sinh(\gamma L)} + \bar{R}, \quad (3.12)$$

whereas for an open boundary at $x=L$ we have

$$U(x) = Z I_{\text{soma}} \frac{\sinh(\gamma[L-x])}{\cosh(\gamma L)} + \bar{R}. \quad (3.13)$$

In the limit $L \rightarrow \infty$, Eq. (3.11) reduces to $U(x) = Z I_{\text{soma}} e^{-\gamma x} + \bar{R}$, showing that the concentration approaches the back-

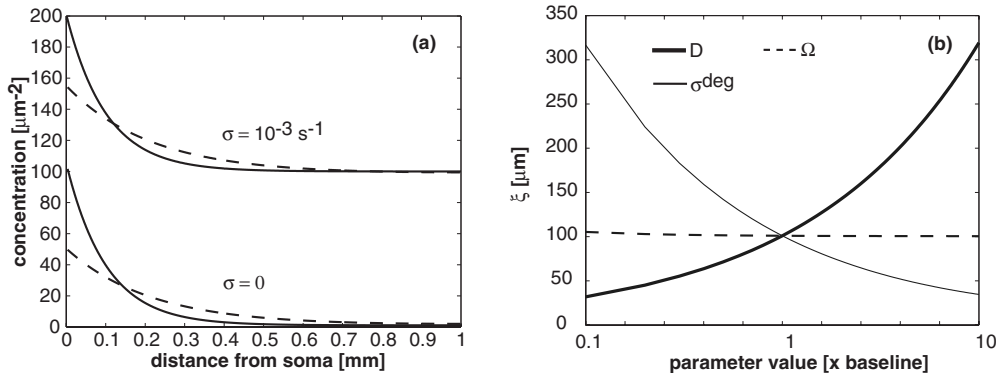


FIG. 2. (a) Steady-state concentration of surface receptors in the dendritic membrane as a function of distance x from the soma. Solid curves show concentration profiles for diffusivity $D=0.1 \mu\text{m}^2 \text{s}^{-1}$ and dashed curves are for $D=0.45 \mu\text{m}^2 \text{s}^{-1}$. Lower two curves are for a zero background concentration, whereas upper two curves are for a nonzero background concentration. The length and circumference of the cable are $L=1 \text{ mm}$ and $l=1 \mu\text{m}$. $N=1000$ identical spines are distributed uniformly along the cable with density $\rho_0=1 \mu\text{m}^{-2}$. The spine parameters are as follows: surface area $A=1 \mu\text{m}^2$, rate of endocytosis $k=10^{-3} \mu\text{m}^2 \text{s}^{-1}$, rate of recycling $\sigma^{\text{rec}}=10^{-3} \text{s}^{-1}$, rate of degradation $\sigma^{\text{deg}}=10^{-5} \text{s}^{-1}$, and hopping rates $\Omega_{\pm}=\Omega=10^{-3} \mu\text{m}^2 \text{s}^{-1}$. The values of most parameters are based on experimental measurements, including the diffusivity [3,4], the rates of constitutive recycling [7,39–41], and the size and density of spines [13], whereas the hopping rate Ω is estimated using a simple model of diffusion within the spine neck [14]. The somatic current is taken to be $I_{\text{soma}}=0.1 \text{ s}^{-1}$ so that the maximum number of synaptic receptors per spine is consistent with experimental observations [42,43]. (b) Space constant ξ as a function of the diffusivity D , the diffusive coupling Ω , and the rate of degradation σ^{deg} .

ground concentration \bar{R} at a rate γ . Thus one can view the space constant ξ as determining the effective range of the diffusive transport of surface receptors from the soma to synaptic targets along the dendrite. It follows that there must be an additional mechanism for supplying distal spines with receptors in the steady state, that is, spines at locations $x \gg \xi$. This is taken into account in our model by including the local source term σ in Eq. (2.6), which maintains the steady-state background concentration \bar{R} ; see Eq. (3.3). Examples of steady-state receptor profiles are shown in Fig. 2(a), and the parameter dependence of the space constant ξ is shown in Fig. 2(b).

Of course the presence of a source of receptors at the soma tends to bias proximal spines (spines adjacent to the soma), particularly when the local source term σ is small [see Fig. 2(a)]. As we have highlighted elsewhere [12,14], this would seem to contradict the notion of *synaptic democracy*, whereby all synapses of a neuron have a similar capacity for influencing the postsynaptic response regardless of location along a dendritic tree [44–46]. Indeed, it has been found experimentally that there is actually an increase in receptor numbers at more distal synapses [47], resulting in a distance-dependent variation in synaptic conductance consistent with somatic equalization. Such behavior could be incorporated into our model by dropping the assumption of identical spines distributed uniformly along the cable. This is also consistent with experimental data indicating that there is considerable amount of heterogeneity in the properties of spines within a single neuron. For example, spine morphology ranges from small filopodial protrusions to large mushroomlike bulbs, and properties such as the surface area of a spine and spine density tend to vary smoothly from proximal to distal locations along the dendrite [13,48,49]. We will return to the issue of heterogeneities in Sec. IV.

B. Branched cable

Let us now consider a branched cable as shown in Fig. 3. It consists of one primary branch of length L_0 and circumference l_0 splitting into two secondary branches with lengths L_1, L_2 and circumferences l_1, l_2 . All branches are assumed to have the same background concentration \bar{R} . A current I_{soma} is injected at the somatic end of the primary branch, whereas the terminal ends of the two secondary branches are closed. By continuity of the surface receptor concentration at the branch point x_B , we can take the corresponding surface concentration U_B to be single valued. It follows from setting $x=0$ in Eq. (3.12) that

$$U_B = Z_j I_j \coth(\gamma_j L_j) + \bar{R}, \quad j = 1, 2, \quad (3.14)$$

where Z_j and γ_j^{-1} are the characteristic impedance and space constant of the j th secondary branch, and I_j is the corresponding current flowing into the branch at point x_B . On the other hand, the membrane potential in the primary branch is

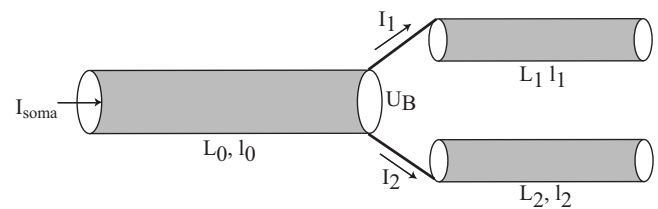


FIG. 3. Schematic diagram of a branched cable consisting of a primary branch with length L_0 and circumference l_0 , and two secondary branches with lengths L_1, L_2 and circumferences l_1, l_2 . The surface receptor concentration U_B at the branch point is continuous, and the diffusive current I_0 flowing through the junction in the primary branch splits into two currents I_1, I_2 .

given by Eq. (3.11) with the terminal impedance $Z_L = (U_B - \bar{R})/I_0$, where I_0 is the current flowing into x_B from the primary branch. Conservation of receptors implies that $I_0 = I_1 + I_2$. Dividing the current conservation equation by $U_B - \bar{R}$ and using Eq. (3.14) then yields

$$\frac{1}{Z_L} = \sum_{j=1,2} \frac{1}{Z_j \coth(\gamma_j L_j)}. \quad (3.15)$$

Following along similar lines to Rall [19], we can now derive the analog of the equivalent-cylinders conditions for receptor trafficking in a branched cable. First, we assume that $\gamma_1 L_1 = \gamma_2 L_2$. (In the context of standard cable theory this would mean that both secondary cables have the same electrotonic length.) Second, we assume that

$$\frac{1}{Z_0} = \frac{1}{Z_1} + \frac{1}{Z_2}, \quad (3.16)$$

that is the characteristic impedances of the three branches are matched. It then follows that $Z_L = Z_0 \coth(\gamma_1 L_1)$. Substituting this expression for Z_L into Eq. (3.11) and performing some algebra leads to the result

$$U(x) = Z_0 I_{\text{soma}} \frac{\cosh(\gamma[L_{\text{eff}} - x])}{\sinh(\gamma L_{\text{eff}})} + \bar{R}, \quad (3.17)$$

where $L_{\text{eff}} = L_0 + \gamma_1 L_1 / \gamma$. Equation (3.17) describes the concentration in a single unbranched cable of effective length L_{eff} and a closed-end boundary condition. In other words, the branched cable has been reduced to a single equivalent cylinder whose other properties are those of the primary branch. Finally, substituting Eq. (3.9) into impedance matching condition (3.16) and assuming that D , $\bar{\Omega}$, and Δ are the same in all branches gives the following relationship between the diameters of the primary and secondary branches:

$$d_0^{1/2} = d_1^{1/2} + d_2^{1/2}. \quad (3.18)$$

Thus, there is one significant difference between the steady-state trafficking model and the corresponding cable model of membrane voltage, namely, that the diameters have to satisfy a $d^{1/2}$ rule rather than Rall's $d^{3/2}$ rule [19].

One could now use the above procedure to collapse a whole dendritic tree to a single equivalent cylinder provided that the following conditions are met: (1) All branches have the same background concentration \bar{R} . (2) All terminal branches have the same boundary conditions and are at the same effective distance from the soma (after rescaling the length of each branch in the tree according to $L_i \rightarrow \gamma_i L_i$). (3) At every branch point the characteristic impedances must be matched, which leads to the $d^{1/2}$ rule when all branches have the same diffusivity D , hopping rate $\bar{\Omega}$, and spine spacing Δ . In general these three conditions will not hold so that one needs an alternative procedure for obtaining the steady-state solution on a tree. Two classes of iterative procedures have been developed within the context of linear cable theory applied to electrically passive and quasiactive dendritic membranes, one based on the graphical calculus of Butz and Cowan [38,50–52] and the other based on the so-called sum-over-trips formalism of Abbott *et al.* [22–25]. Both of these

approaches have been developed within the more general context of time-dependent solutions of the linear cable equation on a tree. In Sec. V we will show how the sum-over-trips method can be extended to our protein trafficking model by using Laplace transforms, which can then be used to derive the steady-state solution on an arbitrary dendritic tree.

IV. DISCRETE SPINES AND HOMOGENIZATION

As we have already indicated, there are several forms of heterogeneity that can modify our calculation of the steady state. Suppose that the various parameters (k , σ^{rec} , σ^{deg} , σ) associated with constitutive recycling are uniform along the cable. This still allows both the density ρ and spine-dendrite coupling Ω_{\pm} to be x dependent. Indeed, the experimentally observed proximal-to-distal variation in the structure and distribution of spines [13,48,49] could be incorporated by taking $\rho(x)$ and $\Omega_{\pm}(x)$ to be continuous functions of x , and this is straightforwardly handled using the continuum model. However, there is also a heterogeneity occurring on a much smaller spatial scale due to the discrete nature of spines, that is, when the spine density is given by Eq. (2.7). There is clearly a separation of length scales between the typical spine spacing Δ of 1 μm and the typical space constant ξ of 100 μm (see Fig. 2); that is, $L \geq \xi \gg \Delta$. This suggests that taking into account the discrete nature of spines will lead to small-scale fluctuations in the steady-state dendritic receptor concentration. We will analyze such fluctuations for a single cable using a multiple-scale homogenization procedure [53], following along similar lines to a recent analysis of the cable equation for voltage and conductance changes along a heterogeneous dendrite [21]. For simplicity, we will ignore heterogeneities on large spatial scales so that the homogenized dendrite reduces to the uniform cable analyzed in Sec. III A.

Introducing the small dimensionless parameter $\varepsilon = \Delta/\xi$, we rewrite Eq. (3.2) in the form

$$\frac{d^2 U}{dx^2} = \rho\left(\frac{x}{\varepsilon}\right) \bar{\Omega}\left(\frac{x}{\varepsilon}\right) \left[U(x) - \bar{R}\left(\frac{x}{\varepsilon}\right) \right] = 0, \quad (4.1)$$

where

$$\rho(y) = \tau^{-1} \sum_{j=1}^N \delta(\varepsilon y - x_j) = \rho_0 \xi \sum_{j=1}^N \delta(y - y_j)$$

and $y_j = x_j/\varepsilon$. We have made explicit the fact that the coupling $\bar{\Omega}$ and background concentration \bar{R} may vary between neighboring spines. As a further simplification, however, we will assume for the moment that $\bar{\Omega}$ and \bar{R} are uniform and that the spines are evenly spaced with $x_j = j\Delta$ and $y_j = j\xi$. Equation (4.1) then becomes

$$\frac{d^2 U}{dx^2} = \left[\bar{\Gamma} + \Delta \Gamma\left(\frac{x}{\varepsilon}\right) \right] [U(x) - \bar{R}] = 0, \quad (4.2)$$

where

$$\bar{\Gamma} = \xi^{-2}, \quad \Delta \Gamma(y) = \bar{\Gamma} \left(\xi \sum_{j=1}^N \delta(y - j\xi) - 1 \right) \quad (4.3)$$

such that $\Delta \Gamma(y)$ is a ξ -periodic function of y .

The basic idea of multiscale homogenization is to expand the solution of Eq. (4.2) as power series in ε , with each term in the expansion depending explicitly on the “slow” (macroscopic) variable x and the “fast” (microscopic) variable $y = x/\varepsilon$:

$$U(x,y) = U_0(x,y) + \varepsilon U_1(x,y) + \varepsilon^2 U_2(x,y) + \cdots, \quad (4.4)$$

where $U_j(x,y)$, with $j=0,1,\dots$, are ξ periodic in y . The perturbation series expansion is then substituted into Eq. (4.2) with x,y treated as independent variables so that derivatives with respect to x are modified according to $\partial_x \rightarrow \partial_x + \varepsilon^{-1} \partial_y$. This generates a hierarchy of equations corresponding to successive powers of ε ,

$$\frac{\partial^2 U_0}{\partial y^2} = 0, \quad (4.5)$$

$$2 \frac{\partial^2 U_0}{\partial x \partial y} + \frac{\partial^2 U_1}{\partial y^2} = 0, \quad (4.6)$$

$$\frac{\partial^2 U_0}{\partial x^2} + 2 \frac{\partial^2 U_1}{\partial x \partial y} + \frac{\partial^2 U_2}{\partial y^2} = [\bar{\Gamma} + \Delta\Gamma(y)][U_0 - \bar{R}] \quad (4.7)$$

at powers $\varepsilon^{-2}, \varepsilon^{-1}, 1$ and

$$\frac{\partial^2 U_n}{\partial x^2} + 2 \frac{\partial^2 U_{n+1}}{\partial x \partial y} + \frac{\partial^2 U_{n+2}}{\partial y^2} = [\bar{\Gamma} + \Delta\Gamma(y)]U_n \quad (4.8)$$

at $O(\varepsilon^n)$, with $n \geq 1$. Define the spatial average of a ξ -periodic function $F(y)$, denoted by $\langle F \rangle$, according to

$$\langle F \rangle = \frac{1}{\xi} \int_0^\xi F(y) dy. \quad (4.9)$$

Since the boundary conditions at the ends $x=0, L$ are independent of ε , we take

$$\left. \frac{d\langle U_n \rangle}{dx} \right|_{x=0} = -\frac{I_s}{LD} \delta_{n,0}, \quad \left. \frac{d\langle U_n \rangle(L)}{dx} \right|_{x=L} = 0, \quad n \geq 0. \quad (4.10)$$

Equation (4.5) implies that U_0 is independent of y , since U_0 should remain bounded in the limit $\varepsilon \rightarrow \infty$. Equation (4.6) and boundedness of U_1 then imply that U_1 is also independent of y . Spatial averaging can now be performed in order to determine the differential equations satisfied by U_0 and U_1 . Taking the spatial average of Eq. (4.7) with $U_0 = \langle U_0 \rangle$ gives

$$\frac{d^2 U_0}{dx^2} = \bar{\Gamma}[U_0 - \bar{R}]. \quad (4.11)$$

We have exploited the fact that U_2 is ξ periodic in y so $\langle \partial^2 U_2 / \partial y^2 \rangle = 0$. Equation (4.11) together with boundary condition (4.10) is precisely the homogeneous equation analyzed in Sec. III A with $\rho \rightarrow \langle \rho \rangle = \rho_0$. Similarly, spatially averaging Eq. (4.8) for $n=1$ shows that U_1 satisfies the equation

$$\frac{d^2 U_1}{dx^2} = \bar{\Gamma} U_1, \quad (4.12)$$

which has the unique solution $U_1=0$ for no-flux boundary condition (4.10). Thus the leading-order corrections arising from small-scale fluctuations in the spine density occur at $O(\varepsilon^2)$. In order to calculate U_2 , we first subtract the averaged Eq. (4.11) from Eq. (4.7) to obtain

$$\frac{\partial^2 U_2}{\partial y^2} = \Delta\Gamma(y)[U_0(x) - \bar{R}]. \quad (4.13)$$

It follows that $U_2(x,y) = [U_0(x) - \bar{R}]\chi(y)$ with $d^2\chi(y)/dy^2 = \Delta\Gamma(y)$ and χ as a ξ -periodic function of y . Integrating once with respect to y gives $\chi'(y) = \chi'(0) + \int_0^y \Delta\Gamma(z) dz$. We can eliminate the unknown $\chi'(0)$ by spatially averaging with respect to y and using $\langle \chi' \rangle = 0$. This gives $\chi'(y) = \oint_0^y \Delta\Gamma(z) dz$ with

$$\oint_0^y f(z) dz \equiv \int_0^y f(z) dz - \left\langle \int_0^y f(z) dz \right\rangle \quad (4.14)$$

for any integrable function f . Another integration with respect to y shows that

$$\chi(y) = \chi(0) + \int_0^y \oint_0^{y'} \Delta\Gamma(z) dz dy'.$$

Spatially averaging this equation in order to express $\chi(0)$ in terms of $\langle \chi \rangle$ and multiplying through by $[U_0(x) - \bar{R}]$ finally gives

$$\begin{aligned} \Delta U_2(x,y) &\equiv U_2(x,y) - \langle U_2 \rangle(x) \\ &= [U_0(x) - \bar{R}] \oint_0^y \oint_0^{y'} \Delta\Gamma(z) dz dy'. \end{aligned} \quad (4.15)$$

It remains to determine the equation satisfied by $\langle U_2 \rangle$. Spatially averaging Eq. (4.8) for $n=2$ gives

$$\frac{d^2 \langle U_2 \rangle}{dx^2} = \bar{\Gamma} \langle U_2 \rangle + \langle \Delta\Gamma(y) U_2(x,y) \rangle. \quad (4.16)$$

Substituting Eq. (4.15) into Eq. (4.16) and reordering the resulting multiple integral yields the result

$$\frac{d^2 \langle U_2 \rangle}{dx^2} = \bar{\Gamma} \langle U_2 \rangle - \left\langle \left(\oint_0^y \Delta\Gamma(z) dz \right)^2 \right\rangle [U_0(x) - \bar{R}]. \quad (4.17)$$

Finally, writing $\langle U \rangle = U_0 + \varepsilon \langle U_2 \rangle + \cdots$ we obtain the homogenized equation (see also [21])

$$\frac{d^2 \langle U \rangle}{dx^2} = \Gamma_\varepsilon [\langle U \rangle - \bar{R}], \quad (4.18)$$

where

$$\Gamma_\varepsilon = \bar{\Gamma} - \varepsilon^2 \left\langle \left(\oint_0^y \Delta\Gamma(z) dz \right)^2 \right\rangle + O(\varepsilon^3). \quad (4.19)$$

The above analysis shows that there are two sources of $O(\varepsilon^2)$ corrections to solution (3.13) of the homogeneous den-

drate. First, the space constant is increased according to

$$\xi \rightarrow \xi_\varepsilon = \xi \left(1 + \frac{\varepsilon^2}{2\bar{\Gamma}} \left\langle \left(\oint_0^y \Delta\Gamma(z) dz \right)^2 \right\rangle \right) + O(\varepsilon^3), \quad (4.20)$$

Second, there are small-scale fluctuations in the dendritic receptor concentration of the form

$$\frac{\Delta U(x,y)}{\langle U \rangle(x)} = \varepsilon^2 \oint_0^y \oint_0^{y'} \Delta\Gamma(z) dz dy' + O(\varepsilon^3). \quad (4.21)$$

It is straightforward to calculate the integrals in Eqs. (4.20) and (4.21) for a periodic spine density [21]:

$$\left\langle \left(\oint_0^y \Delta\Gamma(z) dz \right)^2 \right\rangle = \frac{1}{12\xi^2}, \quad (4.22)$$

$$\oint_0^y \oint_0^{y'} \Delta\Gamma(z) dz dy' = \left[\frac{y}{2\xi} - \frac{y^2}{2\xi^2} - \frac{1}{12} \right]. \quad (4.23)$$

Hence, $\xi_\varepsilon \approx \xi(1 + \varepsilon^2/24)$ and fluctuations in the dendritic receptor concentration vary between $-\varepsilon^2/12$ at spines and $\varepsilon^2/24$ between spines. Clearly, the discrete nature of spines only has a small effect on the receptor concentration provided that $\varepsilon \ll 1$. In terms of physiological parameters [see Eq. (3.5)],

$$\varepsilon = \sqrt{\frac{\Delta}{l}} \sqrt{\frac{\bar{\Omega}}{D}}. \quad (4.24)$$

Since the mean spine spacing Δ and the circumference of the dendritic cable l are both on the order of $1 \mu\text{m}$, it follows that small ε corresponds to a weak effective coupling between the spines and parent dendrite; that is, $\bar{\Omega} \ll D$. The latter condition will hold if $\Omega_\pm \ll D, k(1-\Lambda) \ll D$ [see Eq. (3.3)], which is certainly the case for the basal parameter values used in Fig. 2.

The above multiscale homogenization method can be extended to the case of randomly rather than periodically distributed spines, as well as nonuniform coupling $\bar{\Omega}$, provided that the resulting heterogeneous medium is *ergodic* [54]. That is, the result of averaging over all realizations of the ensemble of spine distributions is equivalent to averaging over the length L of the dendrite in the infinite- L limit. If such an ergodic hypothesis holds and L is sufficiently large so that boundary terms can be neglected, then the above analysis carries over with $\langle \cdot \rangle$ now denoting ensemble averaging. Examples of how to evaluate integrals such as those appearing in Eqs. (4.20) and (4.21) for randomly distributed spines are presented in Ref. [21]. Finally, note that our analysis is easily extended to the full time-dependent model by including a term $D^{-1} \partial U_0 / \partial t$ on the right-hand side of Eq. (4.5) and a term $D^{-1} \partial U_n / \partial t$ on the right-hand side of Eq. (4.8), and performing ε series expansions of $R(x,t)$ and $C(x,t)$. Indeed, the steps of the analysis are almost identical to those of the steady state if the homogenization procedure is carried out after Laplace transforming Eqs. (2.4)–(2.6) along the lines of Sec. V.

V. GREEN'S FUNCTIONS AND LAPLACE TRANSFORMS

In this section we use Laplace transforms to construct Green's functions for the full time-dependent model given by Eqs. (2.4)–(2.6) and its extension to an arbitrary dendritic tree. It will be convenient to fix the units of length to be $1 \mu\text{m}$ and set $A=1$, where A is the surface area of a spine. (R and C then have the same dimensions.) For the sake of illustration, we will assume that the receptor concentrations are in steady state with $I_{\text{soma}}(t)=0$ for $t < 0$. We then determine variations about the steady state induced by a time-dependent somatic current $I_{\text{soma}}(t)=\mathcal{I}(t)$ for $t \geq 0$.

A. Single uniform cable

Consider a single uniform dendritic cable as shown in Fig. 1. The linear response to the time-dependent current $\mathcal{I}(t)$ is given by Eqs. (2.4)–(2.6) with $\sigma=0$ and the initial conditions $U(x,0)=R(x,0)=C(x,0)=0$. Laplace transforming Eqs. (2.4)–(2.6) with $\tilde{U}(x,s)=\int_0^\infty e^{-st} U(x,t) dt$, etc., gives

$$D \frac{d^2 \tilde{U}}{dx^2} - s \tilde{U}(x,s) = \rho_0 [\Omega_+ \tilde{U}(x,s) - \Omega_- \tilde{R}(x,s)] - \frac{1}{l} \tilde{\mathcal{I}}(s) \delta(x), \quad (5.1)$$

and

$$s \tilde{R}(x,s) = [\Omega_+ \tilde{U}(x,s) - \Omega_- \tilde{R}(x,s)] - k \tilde{R}(x,s) + \sigma^{\text{rec}} \tilde{C}(x,s), \quad (5.2)$$

$$s \tilde{C}(x,s) = -\sigma^{\text{rec}} \tilde{C}(x,s) - \sigma^{\text{deg}} \tilde{C}(x,s) + k \tilde{R}(x,s). \quad (5.3)$$

Equation (5.1) is supplemented by the closed boundary conditions

$$\frac{d\tilde{U}(0,s)}{dx} = 0, \quad \frac{d\tilde{U}(L,s)}{dx} = 0. \quad (5.4)$$

Note that we have incorporated the source term at the soma into the diffusion equation itself, rather than in the boundary condition at $x=0$. It is convenient to rewrite Eqs. (5.2) and (5.3) as the matrix equation

$$(\mathbf{M} - s\mathbf{I}) \begin{pmatrix} \tilde{R}(x,s) \\ \tilde{C}(x,s) \end{pmatrix} = - \begin{pmatrix} \Omega_+ \tilde{U}(x,s) \\ 0 \end{pmatrix}, \quad (5.5)$$

with

$$\mathbf{M} = \begin{pmatrix} -k - \Omega_- & \sigma^{\text{rec}} \\ k & -\sigma^{\text{rec}} - \sigma^{\text{deg}} \end{pmatrix}. \quad (5.6)$$

Let μ_\pm denote the eigenvalues of the matrix $-\mathbf{M}$ as

$$\mu_\pm = \frac{1}{2} (k + \Omega_- + \sigma^{\text{rec}} + \sigma^{\text{deg}}) \pm \frac{1}{2} \sqrt{(k + \Omega_- - \sigma^{\text{rec}} - \sigma^{\text{deg}})^2 + 4\sigma^{\text{rec}}k}. \quad (5.7)$$

Solving Eq. (5.5) for \tilde{R}, \tilde{C} in terms of \tilde{U} shows that

$$\begin{aligned} \begin{pmatrix} \tilde{R}(x,s) \\ \tilde{C}(x,s) \end{pmatrix} &= -(\mathbf{M} - s\mathbf{I})^{-1} \begin{pmatrix} \Omega_+ \tilde{U}(x,s) \\ \sigma/s \end{pmatrix} \\ &= \frac{\Omega_+ \tilde{U}(x,s)}{(s + \mu_+)(s + \mu_-)} \begin{pmatrix} s + \sigma^{\text{rec}} + \sigma^{\text{deg}} \\ k \end{pmatrix}. \end{aligned} \quad (5.8)$$

Substituting for $\tilde{R}(x,s)$ into Eq. (5.1) then gives the equation

$$\frac{d^2 \tilde{U}}{dx^2} - \Xi(s) \tilde{U}(x,s) = -\frac{\tilde{I}(x,s)}{D}, \quad (5.9)$$

where

$$\Xi(s) = \frac{s}{D} + \frac{\rho_0 \Omega_+}{D} \left[1 - \Omega_- \frac{s + \sigma^{\text{rec}} + \sigma^{\text{deg}}}{(s + \mu_+)(s + \mu_-)} \right] \quad (5.10)$$

and $\tilde{I}(x,s)$ is the Laplace transform of an effective current density at the soma:

$$\tilde{I}(x,s) = \frac{1}{l} \tilde{I}(s) \delta(x). \quad (5.11)$$

Let $\tilde{\mathcal{G}}(x,y;s)$ denote the Laplace-transformed Green's function, which satisfies the equation

$$\frac{d^2 \tilde{\mathcal{G}}}{dx^2} - \Xi(s) \tilde{\mathcal{G}}(x,y;s) = -\frac{\delta(x-y)}{D}, \quad (5.12)$$

together with the same boundary conditions as $\tilde{U}(x,s)$ for fixed y . A standard calculation yields

$$\begin{aligned} \tilde{\mathcal{G}}(x,y;s) &= \frac{\cosh\{\sqrt{\Xi(s)}[|x-y|-L]\}}{2D\sqrt{\Xi(s)} \sinh[\sqrt{\Xi(s)}L]} \\ &\quad + \frac{\cosh\{\sqrt{\Xi(s)}[x+y-L]\}}{2D\sqrt{\Xi(s)} \sinh[\sqrt{\Xi(s)}L]}. \end{aligned} \quad (5.13)$$

It follows from Eqs. (5.9) and (5.12) that the solution in Laplace space is given by

$$\tilde{U}(x,s) = \int_0^L \tilde{\mathcal{G}}(x,y;s) \tilde{I}(y,s) dy. \quad (5.14)$$

Inverting Eq. (5.14) using the convolution theorem shows that

$$U(x,t) = \int_0^t \int_0^L \mathcal{G}(x,y;t-t') \mathcal{I}(y,t') dy dt', \quad (5.15)$$

with $\mathcal{G}(x,y;t) = \mathcal{L}^{-1} \tilde{\mathcal{G}}(x,y;s)$ as the time-dependent Green's function. Substituting Eq. (5.14) into Eq. (5.8) and applying the convolution theorem then gives the pair of equations

$$R(x,t) = \int_0^t \int_0^L \mathcal{H}(x,y;t-t') \mathcal{I}(y,t') dy dt', \quad (5.16)$$

$$C(x,t) = \int_0^t \int_0^L \mathcal{K}(x,y;t-t') \mathcal{I}(y,t') dy dt'. \quad (5.17)$$

The Green's functions $\mathcal{H}(x,y;t)$ and $\mathcal{K}(x,y;t)$ are obtained by inverting the Laplace transforms

$$\tilde{\mathcal{H}}(x,y;s) = \frac{\Omega_+(s + \sigma^{\text{rec}} + \sigma^{\text{deg}})}{(s + \mu_+)(s + \mu_-)} \tilde{\mathcal{G}}(x,y;s), \quad (5.18)$$

$$\tilde{\mathcal{K}}(x,y;s) = \frac{\Omega_+ k}{(s + \mu_+)(s + \mu_-)} \tilde{\mathcal{G}}(x,y;s). \quad (5.19)$$

The Green's functions \mathcal{G} , \mathcal{H} , and \mathcal{K} determine the linear response of the receptor concentrations to a time-dependent change in the somatic current. More generally, they can be used to calculate the time course of variations in the receptor concentrations following a rapid change in one or more trafficking parameters during the induction of synaptic plasticity, for example. They also have an important probabilistic interpretation. For example, $\mathcal{G}(x,x_0;t)$ can be interpreted as the probability density (per unit length of cable) that a single labeled receptor is at position x in the dendritic membrane at time t given that it was injected at position x_0 at time $t=0$. [Simply set $\mathcal{I}(y,t) = l^{-1} \delta(y-x_0) \delta(t)$.] Similarly, the probability densities for the receptor to be in the surface of a spine or within an intracellular pool are determined by the Green's functions $\mathcal{H}(x,y;t)$ and $\mathcal{K}(x,y;t)$, respectively.

Having calculated the Laplace-transformed Green's functions [see Eqs. (5.13), (5.18), and (5.19)], one can easily recover the steady-state results of Sec. III A by taking $\mathcal{I}(t) = I_{\text{soma}}$ with I_{soma} as a constant so that $\tilde{I}(s) = I_{\text{soma}}/s$. The steady-state solution (if it exists) is given by $U(x) = \lim_{s \rightarrow 0} s \tilde{U}(x,s)$. Applying this to Eq. (5.14) and using Eqs. (5.11) and (5.13), we find that

$$U(x) = \frac{I_{\text{soma}}}{l} \tilde{\mathcal{G}}(x,0;0) = \frac{I_{\text{soma}}}{l} \frac{\cosh\{\sqrt{\Xi(0)}[x-L]\}}{D\sqrt{\Xi(0)} \sinh[\sqrt{\Xi(0)}L]}. \quad (5.20)$$

It is easy to show that $\Xi(0) = \gamma^2$ with γ defined by Eq. (3.5) so that we recover steady-state solution (3.12) in the case $\sigma=0=\bar{R}$. The corresponding steady-state solutions $R(x)$ and $C(x)$ of Eq. (3.1) are obtained by taking the appropriate $s \rightarrow 0$ limit in the Laplace-transformed version of Eqs. (5.16) and (5.17).

Although one cannot write down a simple inversion formula for the Laplace-transformed Green's functions given by Eqs. (5.13), (5.18), and (5.19), fast Fourier transforms provide an efficient method for performing the inversions numerically. Alternatively, in the case of a simple dendritic geometry such as a single cable, it is straightforward to generate the time-dependent Green's functions directly by solving Eqs. (2.4)–(2.6) in the time domain. In Fig. 4, we show example plots of $U(x,t) = \mathcal{G}(x,y;t)$, $R(x,t) = \mathcal{H}(x,y;t)$, and $C(x,t) = \mathcal{K}(x,y;t)$ as functions of x for $y=L/2$ and various times t . These solutions are obtained by numerically solving Eqs. (2.4)–(2.6) for $\sigma=0$, $I_{\text{soma}}=0$ and the initial conditions $U(x,0) = \delta(x-y)$ and $R(x,0) = C(x,0) = 0$. We find that

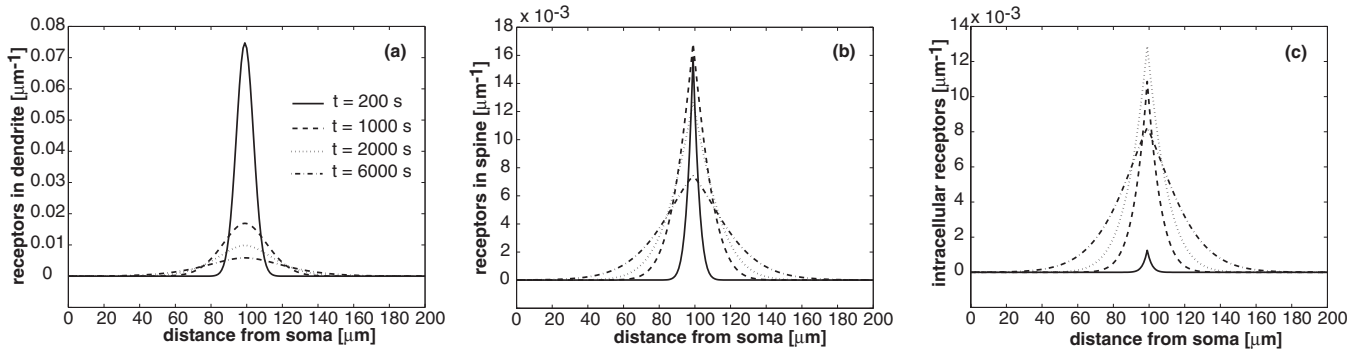


FIG. 4. Time-dependent Green's functions determining response to a surface current injection at the center of a dendritic cable of length $L=200 \mu\text{m}$ and circumference $l=1 \mu\text{m}$. All other parameters are as in Fig. 2. (a) Green's function $\mathcal{G}(x, L/2, t)$ for surface receptors in dendrite plotted as a function of x and various times t . (b) Green's function $\mathcal{H}(x, L/2, t)$ for surface receptors in spines. (c) Green's function $\mathcal{K}(x, L/2, t)$ for receptors in intracellular pools.

$\mathcal{G}(x, L/2; t)$ exhibits subdiffusive behavior, in the sense that its rate of spread across the dendrite is slower than pure diffusion and this cannot be accounted for by a simple rescaling of the diffusivity; see Fig. 5 and Sec. V B. Such an effect is a direct consequence of the diffusive coupling between the dendrite and spines, which act as spatially localized traps. These traps become more effective when there is an asymmetry between the rates of hopping between the dendrite and spines; that is, $\Omega_- < \Omega_+$. As mentioned in Sec. II, this could be due to receptors interacting with scaffolding proteins and cytoskeletal elements within the postsynaptic density located in the spine head. We illustrate the effect of asymmetric coupling in Fig. 6, where Ω_- is reduced by a factor of 10 compared to that in Fig. 4. It can be seen that the Green's function \mathcal{G} is more spatially localized and significantly reduced in amplitude as t increases.

In Fig. 7 we plot time courses for the Green's functions after integrating with respect to position x along the cable, which yields the probabilities of finding a labeled receptor in different states. It can be seen that the probability $\mathcal{P}_U(t) \equiv \int_0^L \mathcal{G}(x, L/2; t) dx$ that the receptor is in the dendritic surface at time t , given that it was in the surface at position $x=L/2$ at time $t=0$, is a monotonically decreasing function of time. On the other hand, the corresponding probabilities to be in a spine or an intracellular pool, $\mathcal{P}_R(t) \equiv \int_0^L \mathcal{H}(x, L/2; t) dx$ and $\mathcal{P}_C(t) \equiv \int_0^L \mathcal{K}(x, L/2; t) dx$, respectively, are unimodal functions of t . The total probability $\mathcal{P}_U(t) + \mathcal{P}_R(t) + \mathcal{P}_C(t)$ is itself a

monotonically decreasing function of t due to receptor degradation. One of the interesting features of the time courses shown in Fig. 7 is that they exhibit processes occurring on different temporal scales. In particular, for the basal parameter values used in Fig. 7(a), there is a relatively rapid change over a time scale of around 30 min in which the probabilities appear to converge to a quasi-steady-state, and a much slower decay over a time scale of many hours. [For our particular choice of parameters, this quasi-steady-state is $\mathcal{P}_U(t) = \mathcal{P}_R(t) = \mathcal{P}_C(t) = 1/3$, which would be the true steady state if $\sigma^{\text{deg}} = 0$.] Increasing the rate of degradation σ^{deg} makes the asymptotic decay faster so that the probabilities do not reach a quasi-steady-state; see Fig. 7(b). Interestingly, the existence of multiple time scales might help resolve conflicting experimental results regarding the effective rate of constitutive recycling. A variety of optical, biochemical, and electrophysiological studies of AMPA receptors in hippocampal neurons [7,39,40] indicate that the rate of constitutive recycling is relatively fast (around 30 min), whereas a recent photoinactivation study of Adesnik *et al.* [26] suggests that while recovery of surface receptors at the soma is fast, recovery of AMPA receptors at dendritic synapses is much slower (~ 16 h). Our mathematical analysis suggests that there could be both fast and slow components of recovery following inactivation of receptors, even when the rates of constitutive recycling are relatively fast. Additional time scales are introduced if the binding of receptors to scaffolding proteins is taken into account [14].

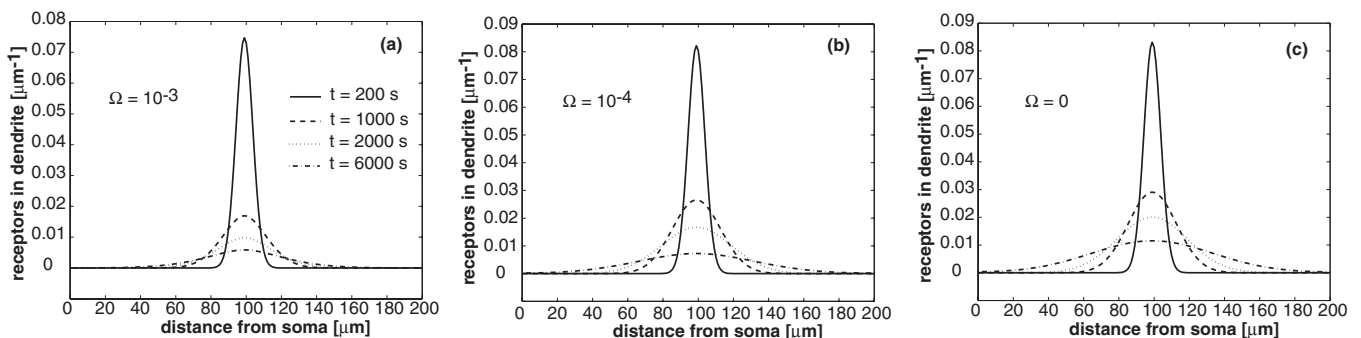


FIG. 5. Plots of time-dependent Green's function $\mathcal{G}(x, L/2, t)$ for different values of the diffusive coupling Ω . (a) Same as Fig. 4(a) with $\Omega = 10^{-3} \mu\text{m}^2 \text{s}^{-1}$. (b) $\Omega = 10^{-4} \mu\text{m}^2 \text{s}^{-1}$. (c) Zero diffusive coupling between dendrite and spines (pure diffusion).

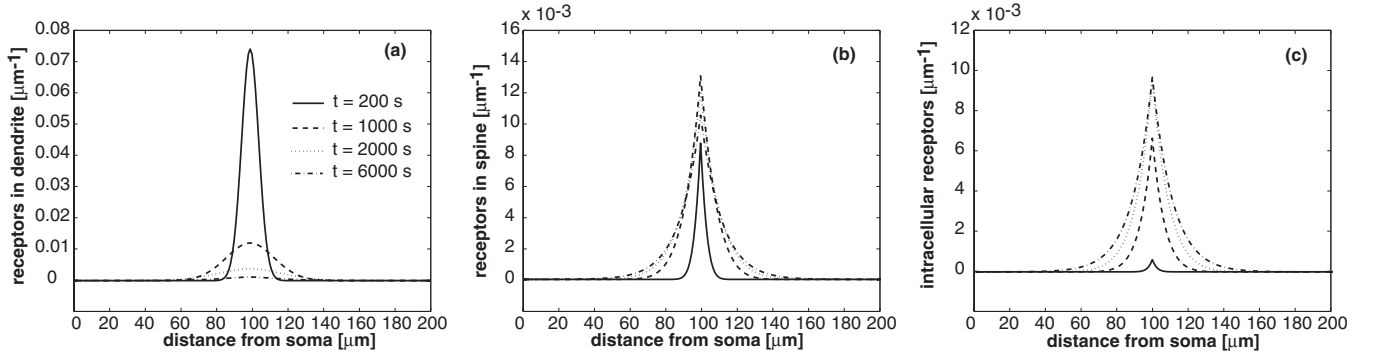


FIG. 6. Same as Figs. 4(a)–4(c) except that $\Omega_- = 0.1\Omega_+ = 10^{-4} \mu\text{m}^2 \text{s}^{-1}$.

B. Large- t behavior

A useful aspect of Laplace transforms is that the small- s limit provides information about the asymptotic behavior of time-dependent solutions in the large- t limit. The large- t behavior of the time-dependent Green's function $\mathcal{G}(x, y; t)$ determines the asymptotic rate at which the dendritic receptor concentration $U(x, t)$ relaxes to the steady state in the case of a constant somatic current. It also determines the asymptotic decay of the probabilities shown in Fig. 7. For the sake of illustration, we set $y=0$ and consider a semi-infinite cable whose Laplace-transformed Green's function is obtained by taking the limit $L \rightarrow \infty$ in Eq. (5.13):

$$\tilde{\mathcal{G}}(x, 0; s) = \frac{1}{D\sqrt{\Xi(s)}} e^{-\sqrt{\Xi(s)}x}, \quad x \geq 0.$$

We will characterize the long-time behavior in terms of moments of the Green's function defined according to

$$M_n(t) = \int_0^\infty x^n \mathcal{G}(x, 0; t) dx. \quad (5.21)$$

In particular, $M_0(t)$ is the probability $\mathcal{P}_U(t)$ that an individual receptor is located within the dendritic membrane at time t given that it was injected at $x=0$ at time $t=0$; see Sec. V A. Taking Laplace transforms shows that

$$\tilde{M}_n(s) \equiv \int_0^\infty x^n \tilde{\mathcal{G}}(x, s) dx = \frac{n!}{D\Xi^{1+n/2}(s)}. \quad (5.22)$$

The small- s behavior of $\tilde{M}_n(s)$ can be used to determine the large- t behavior of $M_n(t)$ by invoking the following theorem [55]:

Theorem 1. (Strong Tauberian theorem for the Laplace transform) If $f(t) \geq 0$, $f(t)$ is ultimately monotonic as $t \rightarrow \infty$, F is slowly varying at infinity, and $0 < \alpha < \infty$, then each of the relations

$$\tilde{f}(s) = \int_0^\infty e^{-st} f(t) dt \sim F(1/s) s^{-\alpha} \quad \text{as } s \rightarrow 0$$

and

$$f(t) \sim \frac{t^{\alpha-1} F(t)}{\Gamma(\alpha)} \quad \text{as } t \rightarrow \infty$$

implies the other. Here $\Gamma(\alpha)$ denotes the gamma function.

First, note that $\Xi(s) = 0$ is a cubic with roots $s = -\lambda_j$, where $j=1, 2, 3$, so that we can write

$$\Xi(s) = \frac{(s + \lambda_1)(s + \lambda_2)(s + \lambda_3)}{D(s + \mu_+)(s + \mu_-)}.$$

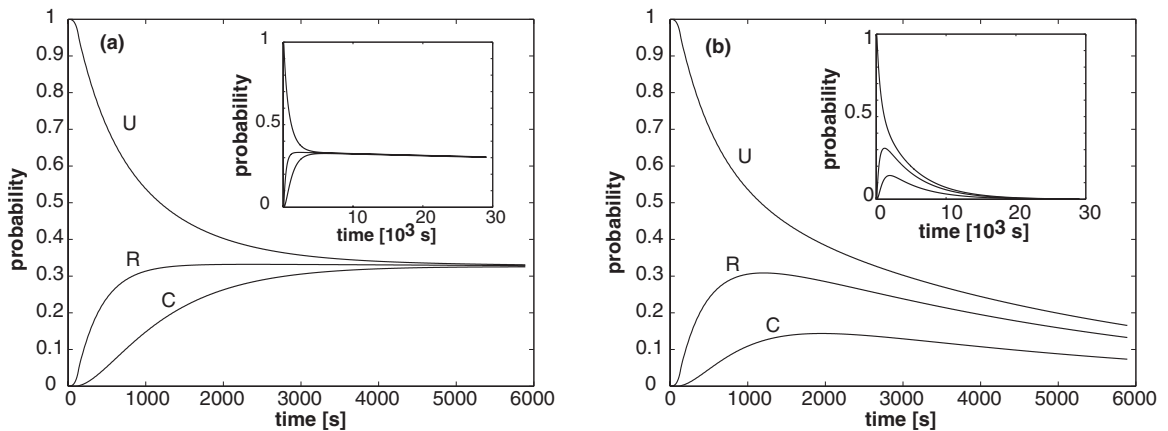


FIG. 7. Time courses of probabilities $\mathcal{P}_U(t), \mathcal{P}_R(t), \mathcal{P}_C(t)$ associated with dendritic surface, spines, and intracellular stores, respectively. (a) Same parameters as in Fig. 4 with $\sigma^{\text{deg}} = 10^{-5} \text{ s}^{-1}$. (b) Same as (a) except for a faster rate of degradation $\sigma^{\text{deg}} = 10^{-3} \text{ s}^{-1}$. Insets show same plots over a longer time interval.

Let us order the roots by taking $0 \leq \lambda_1 < \lambda_2 < \lambda_3$ and define the function $H(s)$ according to $H(s) = \Xi(s - \lambda_1)/s$. Using the Tauberian theorem together with $\mathcal{L}^{-1}\tilde{f}(s+a) = e^{-at}\mathcal{L}^{-1}\tilde{f}(s)$, we then find that

$$M_n(t) = e^{-\lambda_1 t} \mathcal{L}^{-1} \left[\frac{n!}{s^{1+n/2} H(s)^{1+n/2} D} \right] \sim e^{-\lambda_1 t} \frac{n! t^{n/2}}{\Gamma(1+n/2) H(0)^{1+n/2} D}, \quad t \rightarrow \infty, \quad (5.23)$$

with

$$H(0) = \frac{(\lambda_2 - \lambda_1)(\lambda_3 - \lambda_1)}{D(\mu_+ - \lambda_1)(\mu_- - \lambda_1)}.$$

We find that $\lambda_1 < \mu_- < \lambda_2 < \mu_+ < \lambda_3$ so $H(0) > D^{-1}$.

The zeroth-order moment varies asymptotically as $M_0(t) \sim e^{-\lambda_1 t}/DH(0)$. If the spines were decoupled from the dendrite ($\Omega_{\pm} = 0$), then $\lambda_1 = 0$ and $H(0) = 1/D$ so that $M_0(t) = 1$ for all t . In other words, the receptor injected into the dendritic surface at $t=0$ remains in the surface. On the other hand, if $\Omega_{\pm} > 0$ and the rate of degradation $\sigma^{\text{deg}} > 0$, then $\lambda_1 > 0$ so that the probability of being in the surface decays exponentially with time, reflecting the fact that the receptor is eventually degraded. A third possibility is that $\Omega_{\pm} > 0$ and $\sigma^{\text{deg}} = 0$. In this case, $\lambda_1 = 0$ but $H(0) > 1/D$ so that $M_0(t) \rightarrow [DH(0)]^{-1} < 1$ as $t \rightarrow \infty$. It follows that $1 - [DH(0)]^{-1}$ is the asymptotic probability that the receptor is in a spine or an intracellular pool rather than in the dendritic membrane. Given that $M_0(t) < 1$, it is useful to define the conditional moments

$$\mathcal{M}_n(t) = \frac{M_n(t)}{M_0(t)} \sim \frac{n! t^{n/2}}{\Gamma(1+n/2) H(0)^{n/2}}, \quad t \rightarrow \infty. \quad (5.24)$$

The first moment $\mathcal{M}_1(t)$ determines the progress of the receptor along the dendritic cable, whereas $\Delta\mathcal{M}(t) \equiv \mathcal{M}_2(t) - \mathcal{M}_1(t)^2$ determines the variance in its position. Of course, the net motion along the cable is not due to ballistic transport but is a consequence of diffusion with a reflecting boundary at $x=0$. In the limit $t \rightarrow \infty$ we have

$$\mathcal{M}_1(t) \sim 2 \sqrt{\frac{t}{\pi H(0)}}, \quad \Delta\mathcal{M}(t) \sim \left(2 - \frac{4}{\pi}\right) \frac{t}{H(0)}. \quad (5.25)$$

The $H(0)$ factors take into account the fact that the dendritic spines act as traps for the diffusing receptor, thus reducing the mean and variance of its displacement. In Fig. 8 we illustrate how both the asymptotic relaxation rate λ_1 and the scale factor $H(0)$ vary with the rate of degradation σ^{deg} . The relaxation rate λ_1 is a monotonically increasing function of σ^{deg} , and its range of values is consistent with the asymptotic time courses shown in the insets of Fig. 7. Moreover, $DH(0) \rightarrow 3$ as $\sigma^{\text{deg}} \rightarrow 0$, consistent with the quasi-steady-state shown in Fig. 7(a).

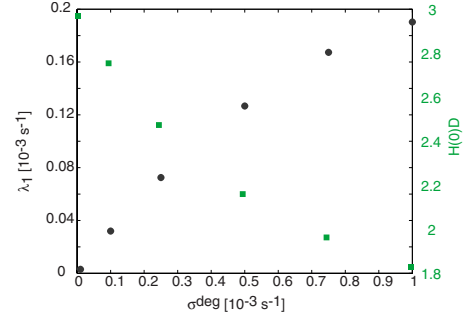


FIG. 8. (Color online) Plot of asymptotic relaxation rate λ_1 (filled circles) and scaling factor $H(0)D$ (filled squares) as a function of the rate of degradation σ^{deg} . All other parameter values are as in Fig. 2.

C. Sum-over-trips on dendritic trees

Another useful feature of Laplace transforms is that they provide an efficient method for evaluating the Green's function on a more complex dendritic tree structure such as the one shown schematically in Fig. 9. Let \mathcal{T} denote the set of all branches in the tree, which are labeled by the index $i \in \mathcal{T}$. We assume (i) each branch is a uniform cable, (ii) all terminal nodes are closed, and (iii) continuity of receptor concentration and conservation of current at all branch nodes. It will be convenient to choose coordinates such that a branch node is at the point $x=0$ on all branches radiating from that node. Applying Laplace transforms to the receptor concentrations in the j th branch as outlined in Sec. V A leads to an equation of the form

$$\frac{d^2 \tilde{U}_j}{dX^2} - \tilde{U}_j(X, s) = -\frac{\tilde{\mathcal{I}}_j(X, s)}{D}, \quad 0 \leq X \leq \mathcal{L}_j(s), \quad (5.26)$$

where we have performed the rescalings $x \rightarrow X = \gamma_j(s)x$ and $L_j \rightarrow \mathcal{L}_j(s) = \gamma_j(s)L_j$, with $\gamma_j(s) = \sqrt{\Xi_j(s)}$ and $\Xi_j(s)$ defined by Eq. (5.10) for j -dependent spine and cable parameters. The diffusivity D is taken to be the same in all branches, which is reasonable given the size of receptors compared to the surface area of even small dendrites. As in the single cable case,

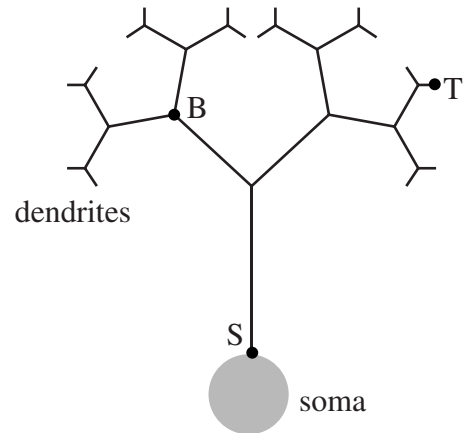


FIG. 9. Schematic diagram of a branched dendritic tree showing a branch node B , a terminal node T , and the special terminal node S adjoining the soma.

$\tilde{\mathcal{I}}_j(X, s)$ represents the Laplace transform of a current density which takes into account the current I_{soma} at the soma and the local supply of receptors in intracellular pools. If we ignore the latter, then

$$\tilde{\mathcal{I}}_j(X, s) = \frac{\tilde{\mathcal{I}}(s)}{l} \delta(X - \mathcal{L}_0(s)) \delta_{j,0}, \quad (5.27)$$

with the main branch labeled by $i=0$. Continuity of receptor concentration at a branch node requires

$$\tilde{U}_i(0, s) = \tilde{U}_j(0, s) \quad (5.28)$$

for all pairs (i, j) radiating from the node. Similarly, current conservation requires that

$$\sum_j z_j(s) \left. \frac{\partial \tilde{U}_j}{\partial X} \right|_{X=0} = 0, \quad z_j(s) = l_j D \gamma_j(s), \quad (5.29)$$

where the sum is over all branches j connected to the node. Note that $z_j(0)$ is the inverse of the characteristic impedance Z_j defined by Eq. (3.9). Finally, we have the boundary condition

$$\left. \frac{\partial \tilde{U}_j}{\partial X} \right|_{X=\mathcal{L}_j} = 0, \quad (5.30)$$

for all terminal branches j including the main branch.

The general solution of Eq. (5.26) can be written in the form

$$\tilde{U}_i(X, s) = \sum_{j \in \mathcal{T}} \int_0^{\mathcal{L}_j(s)} G_{ij}(X, Y; s) \tilde{\mathcal{I}}_j(Y, s) dY, \quad (5.31)$$

where the Green's function $G_{ij}(X, Y; s)$ satisfies the homogeneous equation

$$\frac{d^2 G_{ij}(X, Y; s)}{dX^2} - G_{ij}(X, Y; s) = -\frac{1}{D} \delta_{i,j} \delta(X - Y), \quad (5.32)$$

with the same boundary conditions as $\tilde{U}_i(X, s)$ for fixed j, Y . Following the sum-over-trips method of Abbott *et al.* [22,23], particularly the version applied recently to quasi-active dendrites [25], it can be shown that for a general tree the corresponding Green's function has an infinite series expansion in terms of the corresponding Green's function $G_\infty(X)$ for an infinite cable:

$$G_{ij}(X, Y; s) = \sum_{\text{trips}} A_{\text{trip}}(s) G_\infty(\mathcal{L}_{\text{trip}}(i, j, X, Y, s)), \quad (5.33)$$

where

$$G_\infty(X) = \frac{e^{-|X|}}{2D}, \quad (5.34)$$

and $\mathcal{L}_{\text{trip}}(i, j, X, Y, s)$ is the length (in rescaled coordinates) of a path along the tree starting at point X on branch i and ending at point Y on branch j . The sum in Eq. (5.33) is restricted to a set of paths or *trips* that are constructed using the following rule [22]:

A trip from (X, i) to (Y, j) may start out in either direction along branch i but it can subsequently change direction only

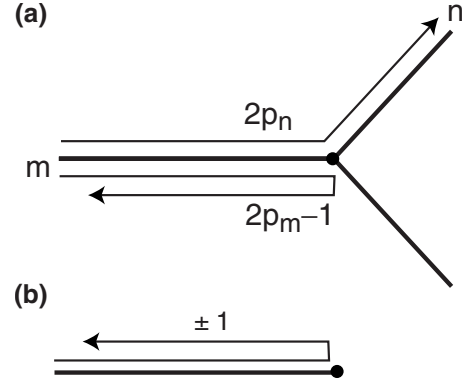


FIG. 10. Schematic diagram showing amplitude factors picked up by a trip on reaching (a) a branch node and (b) a terminal node.

at a branch or terminal node. A trip is always reflected back at a terminal node, whereas at a branch node it may be transmitted to another branch or reflected back. A trip may pass through the points (X, i) and (Y, j) an arbitrary number of times as long as it starts at (X, i) and ends at (Y, j) .

For each trip, the associated amplitude $\mathcal{A}_{\text{trip}}$ is calculated according to the following rules:

- (1) Initially take $\mathcal{A}_{\text{trip}}(s) = 1$.
- (2) For every branch node at which the trip passes from an initial segment m to a different segment n , $n \neq m$, multiply $\mathcal{A}_{\text{trip}}(s)$ by a factor of $2p_n(s)$; see Fig. 10(a).
- (3) For every branch node at which the trip is reflected back along the same segment m , multiply $\mathcal{A}_{\text{trip}}(s)$ by a factor of $2p_m(s) - 1$; see Fig. 10(a).
- (4) For every closed (open) terminal node, multiply $\mathcal{A}_{\text{trip}}(s)$ by a factor of $+1$ (-1); see Fig. 10(b).
- (5) Multiply $\mathcal{A}_{\text{trip}}(s)$ by an additional factor of 2 if a trip starts or ends on a closed terminal node. (This factor is usually not mentioned explicitly in the sum-over-trips rules, but see Ref. [24].)

Here the factor p_m is given by

$$p_m(s) = \frac{z_m(s)}{\sum_n z_n(s)}, \quad (5.35)$$

where the sum is over all branches n radiating from a given branch node and $z_m(s)$ is defined according to Eq. (5.29).

In order to obtain the solution in the time domain, it is first necessary to express Eq. (5.31) in physical coordinates:

$$\tilde{U}_i(x, s) = \sum_{j \in \mathcal{T}} \int_0^{L_j} \tilde{G}_{ij}(x, y; s) \tilde{\mathcal{I}}_j(y, s) dy, \quad (5.36)$$

with

$$\tilde{G}_{ij}(x, y; s) = \frac{G_{ij}(\gamma_i(s)x, \gamma_j(s)y; s)}{\gamma_j(s)}. \quad (5.37)$$

Applying the inverse Laplace transform then gives the general solution for the surface receptor concentration in an arbitrary dendritic tree:

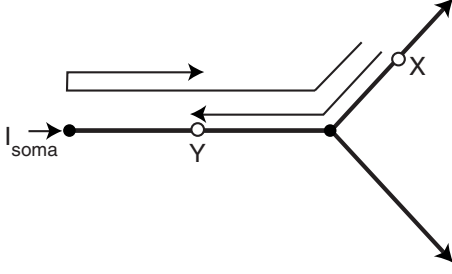


FIG. 11. Simple configuration consisting of one main branch and two semi-infinite secondary branches. Two shortest trips starting at X and ending at Y are shown.

$$U_i(x, t) = \sum_{j \in T} \int_0^t \mathcal{G}_{ij}(x, y; t - t') \mathcal{I}_j(y, t') dy dt', \quad (5.38)$$

with $\mathcal{G}_{ij}(x, y; t) = \mathcal{L}^{-1} \tilde{\mathcal{G}}_{ij}(x, y; s)$. The time-dependent Green's function $\mathcal{G}_{ij}(x, y; t)$ can be interpreted as the probability that a receptor is at location x in the surface of the i th branch at time t , given that it was initially injected into the surface at location y of the j th branch at time $t=0$. Moreover, as in the case of a single cable (Sec. V A), the steady-state Green's function is given by $\tilde{\mathcal{G}}_{ij}(x, y; 0)$ with $\gamma_j(0) = \sqrt{\Xi(0)}$ as the inverse space constant of the j th branch; see Eq. (3.5). Having constructed the Green's function for dendritic surface receptors, it is straightforward to write down the corresponding Green's functions for receptors in spines and intracellular stores using Eqs. (5.18) and (5.19):

$$\tilde{\mathcal{H}}_{ij}(x, y; s) = \frac{\Omega_{+,i}(s + \sigma_i^{\text{rec}} + \sigma_i^{\text{deg}})}{(s + \mu_{+,i})(s + \mu_{-,i})} \tilde{\mathcal{G}}_{ij}(x, y; s), \quad (5.39)$$

$$\tilde{\mathcal{K}}_{ij}(x, y; s) = \frac{\Omega_{+,i} k_i}{(s + \mu_{+,i})(s + \mu_{-,i})} \tilde{\mathcal{G}}_{ij}(x, y; s). \quad (5.40)$$

As an illustrative example, consider the configuration shown in Fig. 11, in which the main branch $j=0$ of finite length L_0 bifurcates into two semi-infinite secondary branches labeled $j=1, 2$. A trip starting at point X in branch 1 and ending at point Y in the main branch has to pass through the branch point exactly once, picking up a factor of $2p_0$. There are two basic trips, one that goes straight to Y with $\mathcal{L}_{\text{trip}} = X + Y$, and the other that reflects once off the terminal node before ending at Y so that $\mathcal{L}_{\text{trip}} = X + 2L_0 - Y$. Each of these two trips is associated with an infinite set of other trips involving q reflections at the terminal and branching nodes, $q \geq 1$, thus resulting in an additional trip length $2qL_0$ and an additional amplitude factor $(2p_0 - 1)^q$. Summing over q gives

$$G_{10}(X, Y; s) = \frac{p_0(s)}{D} \frac{e^{-(X+Y)} + e^{-[X+2L_0(s)-Y]}}{1 - [2p_0(s) - 1]e^{-2L_0(s)}}. \quad (5.41)$$

It follows that the steady-state Green's function is given by

$$\tilde{G}_{10}(x, y; 0) = \frac{p_0(0)}{D\gamma_0} \frac{e^{-(\gamma_1 x + \gamma_0 y)} + e^{-[\gamma_1 x + \gamma_0(2L_0 - y)]}}{1 - [2p_0(0) - 1]e^{-2\gamma_0 L_0}}. \quad (5.42)$$

Note that if $z_0(0) = z_1(0) + z_2(0)$, which is equivalent to impedance matching condition (3.16), then $p_0 = 1/2$ and we recover the equivalent-cylinders result of Sec. III B.

For more complex tree configurations, it is possible to carry out partial summations over trips in Eq. (5.33) but the resulting expression tends to be unwieldy [24]. On the other hand, for sufficiently large s , one can truncate the series to include a relatively small number of trips and then carry out a numerical inversion of the Laplace transform (see [23,25] for further discussions of numerical implementations). This will determine the behavior of the solution up to some finite time t . The sum-over-trips method is less useful if one is interested in the long-time asymptotic behavior of solutions, that is, the small- s behavior of the Laplace-transformed Green's function. It is then more useful to use an alternative approach based on integral equations [56]. That is, one can solve the original diffusion-trapping equations on each branch separately using Green's theorem, which yields a set of coupled integral equations involving the unknown solutions at the branch nodes of the tree. The latter are then determined self-consistently by imposing current conservation at each branch node and using Laplace transforms. This generates a closed expression for the Laplace-transformed Green's function in the form of a continued fraction, which can then be used to extract the long-time behavior of solutions. It can also be used to calculate the mean first passage time for a single receptor to reach a synaptic target from the soma [12]. The continued fraction has a naturally recursive form, which is particularly useful for analyzing self-similar structures such as Cayley trees [56].

VI. DISCUSSION

In this paper we showed how the trafficking of protein receptors along the surface of a spiny dendritic tree can be described in terms of a continuum model that is similar in structure to the linear cable equation for the electrical potential in quasiactive dendritic membranes. This allowed us to apply Green's function and transform methods in order to calculate the steady-state and time-dependent receptor concentrations along single and branched dendritic cables. In particular, we derived the Green's function for the diffusive transport of receptors within the dendritic membrane and used this to explore the effects of trapping within spines. We showed how trapping leads to subdiffusive behavior and that relaxation to the steady state involves multiple time scales arising from the receptor dynamics within spines. We also used homogenization theory to derive corrections to the continuum model due to the discrete nature of spines, and established that such corrections are small provided that the diffusive coupling between dendrites and spines is sufficiently weak.

In conclusion, we have shown how cable theory provides a general theoretical framework for exploring the role of lateral membrane diffusion in the transport of protein receptors

in neurons. There are a number of ways in which our work may be extended. The first concerns a more detailed single-spine model in which interactions between receptors and scaffolding proteins within the PSD are taken into account [27,28]. This introduces nonlinearities into the single-spine dynamics associated with the kinetics of receptor binding to scaffolding proteins. In order to apply Laplace-transform methods it is then necessary to linearize the single-spine dynamics, which is a reasonable approximation if the binding sites are unsaturated, for example. Another important extension is to consider the effects of noise. In our continuum model we take the state variable of a single spine to be a receptor concentration and formulate the single-spine dynamics in terms of a system of kinetic equations. This implicitly assumes that the number of receptors within a spine is sufficiently large; otherwise random fluctuations about the mean receptor number may become significant. Typically the size of fluctuations varies as $1/\sqrt{N}$, where N is the number of receptors. One way to take into account the inherent stochasticity or “intrinsic noise” arising from fluctuations in receptor number is to replace the kinetic equations by a corresponding

master equation [57], which describes the temporal evolution of the probability distribution for the receptors within the spine. Performing some form of small fluctuation expansion would lead to a stochastic version of our continuum model, which could then be analyzed using Green’s-function techniques along the lines of the stochastic cable equation [58]. Finally, it would be interesting to develop a higher-dimensional version of our diffusion-trapping model in which molecules are free to diffuse throughout the volume of a dendrite but can become trapped by spines on the membrane surface. A recent experimental and computational study of molecular diffusion within the dendrites of Purkinje cells suggests that the temporary confinement in spines leads to anomalous diffusion on short time scales and reduced normal diffusion on longer time scales [59].

ACKNOWLEDGMENT

This work was supported by the National Science Foundation (Grant No. DMS 0813677).

-
- [1] D. Choquet and A. Triller, *Nat. Rev. Neurosci.* **4**, 251 (2003).
 [2] A. Triller and D. Choquet, *Trends Neurosci.* **28**, 133 (2005).
 [3] L. Groc, M. Heine, L. Cognet, K. Brickley, F. A. Stephenson, B. Lounis, and D. Choquet, *Nat. Neurosci.* **7**, 695 (2004).
 [4] M. C. Ashby, S. R. Maier, A. Nishimune, and J. M. Henley, *J. Neurosci.* **26**, 7046 (2006).
 [5] M. D. Ehlers, M. Heine, L. Groc, M.-C. Lee, and D. Choquet, *Neuron* **54**, 447 (2007).
 [6] T. M. Newpher and M. D. Ehlers, *Neuron* **58**, 472 (2008).
 [7] M. D. Ehlers, *Neuron* **28**, 511 (2000).
 [8] D. S. Bredt and R. A. Nicoll, *Neuron* **40**, 361 (2003).
 [9] G. L. Collingridge, J. T. R. Isaac, and Y. T. Wang, *Nat. Rev. Neurosci.* **5**, 952 (2004).
 [10] V. A. Derkach, M. C. Oh, E. S. Guire, and T. R. Soderling, *Nat. Rev. Neurosci.* **8**, 101 (2007).
 [11] P. C. Bressloff, B. A. Earnshaw, and M. J. Ward, *SIAM J. Appl. Math.* **68**, 1223 (2008).
 [12] P. C. Bressloff and B. A. Earnshaw, *Phys. Rev. E* **75**, 041915 (2007).
 [13] K. E. Sorra and K. M. Harris, *Hippocampus* **10**, 501 (2000).
 [14] B. A. Earnshaw and P. C. Bressloff, *J. Comput. Neurosci.* **25**, 366 (2008).
 [15] *The Theoretical Foundations of Dendritic Function: Selected Papers of Wilfrid Rall with Commentaries*, edited by I. Segev, J. Rinzel, and G. M. Shepherd (MIT Press, Cambridge, 1995).
 [16] A. Zador and C. Koch, *J. Neurosci.* **14**, 4705 (1994).
 [17] C. Koch, *Biophysics of Computation* (Oxford University Press, Oxford, 1999).
 [18] G. Stuart, N. Spruston, and M. Hausser, *Dendrites* (Oxford University Press, Oxford, 2007).
 [19] W. Rall, *Ann. N.Y. Acad. Sci.* **96**, 1071 (1962).
 [20] W. Rall, in *Neural Theory and Modeling*, edited by R. F. Reiss (Stanford University Press, Palo Alto, 1964), p. 73.
 [21] C. Meunier and B. L. d’Incamps, *Neural Comput.* **20**, 1732 (2008).
 [22] L. F. Abbott, E. Fahri, and S. Gutmann, *Biol. Cybern.* **66**, 49 (1991).
 [23] B. J. Cao and L. F. Abbott, *Biophys. J.* **64**, 303 (1993).
 [24] P. C. Bressloff, V. M. Dwyer, and M. J. Kearney, *J. Phys. A* **29**, 1881 (1996).
 [25] S. Coombes, Y. Timofeeva, C. M. Svensson, G. J. Lord, K. Josic’, S. J. Cox, and C. M. Colbert, *Biol. Cybern.* **97**, 137 (2007).
 [26] H. Adesnik, R. A. Nicoll, and P. M. England, *Neuron* **48**, 977 (2005).
 [27] B. A. Earnshaw and P. C. Bressloff, *J. Neurosci.* **26**, 12362 (2006).
 [28] D. Holcman and A. Triller, *Biophys. J.* **91**, 2405 (2006).
 [29] J. R. Cooney, J. L. Hurlburt, D. K. Selig, K. M. Harris, and J. C. Fiala, *J. Neurosci.* **22**, 2215 (2002).
 [30] For simplicity we assume that spines do not share intracellular stores of receptors. However, Cooney *et al.* [29] found that endosomes, the intracellular compartments responsible for the sorting of receptors for recycling or degradation, can be shared by up to 20 spines. Including endosomal sharing in our model would create a potential source of nonlocal interaction between spines. However, the range of such interactions arising from endosomal sharing (10–20 μm) is relatively small compared to the space constant of lateral receptor diffusion. Moreover, one could reinterpret the spine density $\rho(x)$ in terms of clusters of spines, each of which shares a distinct intracellular pool. We also assume that recycling occurs between intracellular pools and spines rather than the surface of the dendritic cable. This is motivated by experimental data that find hotspots for receptor endocytosis in domains adjacent to the postsynaptic density within spines [41]. However, our model is easily modified to allow for a direct recycling of receptors within the dendritic membrane.

- [31] C.-H. Kim and J. E. Lisman, *J. Neurosci.* **21**, 4188 (2001).
- [32] M. Setou, D. H. Seog, Y. Tanaka, Y. Kanai, Y. Takei, and N. Hirokawa, *Nature (London)* **417**, 83 (2002).
- [33] R. Kelleher III, A. Govindarajan, and S. Tonegawa, *Neuron* **44**, 59 (2004).
- [34] W. Ju, W. Morishita, J. Tsui, G. Gaietta, T. J. Deerinck, S. R. Adams, C. C. Garner, R. Y. Tsien, M. H. Ellisman, and R. C. Malenka, *Nat. Neurosci.* **7**, 244 (2004).
- [35] M. A. Sutton and E. M. Schuman, *J. Neurobiol.* **64**, 116 (2005).
- [36] J. J. B. Jack, D. Noble, and R. Tsien, *Electrical Current Flow in Excitable Cells*, 2nd ed. (Clarendon, Oxford, 1983).
- [37] W. R. Holmes and W. Rall, *J. Neurophysiol.* **68**, 1421 (1992).
- [38] E. G. Butz and J. D. Cowan, *Biophys. J.* **14**, 661 (1974).
- [39] C. Luscher, H. Xia, E. C. Beattie, R. C. Carroll, M. von Zastrow, and R. C. Malenka, *Neuron* **24**, 649 (1999).
- [40] M. Passafaro, V. Piech, and M. Sheng, *Nat. Neurosci.* **4**, 917 (2001).
- [41] T. A. Blanpied, D. B. Scott, and M. D. Ehlers, *Neuron* **36**, 435 (2002).
- [42] Z. Nusser, R. Lujan, L. Laube, J. D. B. Roberts, E. Molnar, and P. Somogyi, *Neuron* **21**, 545 (1998).
- [43] J. I. Tanaka, M. Matsuzaki, E. Tarusawa, A. Momiyama, E. Molnar, H. Kasai, and R. Shigemoto, *J. Neurosci.* **25**, 799 (2005).
- [44] M. Hausser, *Curr. Biol.* **11**, R10 (2001).
- [45] C. C. Rumsey and L. F. Abbott, *J. Neurophysiol.* **96**, 2307 (2006).
- [46] Y. Timofeeva, S. J. Cox, S. Coombes, and J. Josic', *J. Comput. Neurosci.* **25**, 228 (2008).
- [47] J. C. Magee and E. P. Cook, *Nat. Neurosci.* **3**, 895 (2000).
- [48] E. A. Nimchinsky, B. L. Sabatini, and K. Svoboda, *Annu. Rev. Physiol.* **64**, 313 (2002).
- [49] S. Konur, D. Rabinowitz, V. L. Fenstermaker, and R. Yuste, *J. Neurobiol.* **56**, 95 (2003).
- [50] B. Horwitz, *Biophys. J.* **36**, 155 (1981).
- [51] C. Koch and T. Poggio, *J. Neurosci. Methods* **12**, 303 (1985).
- [52] W. R. Holmes, *Biol. Cybern.* **55**, 115 (1986).
- [53] G. A. Pavliotis and A. M. Stuart, *Multiscale Methods: Averaging and Homogenization* (Springer, New York, 2007).
- [54] S. Torquato, *Random Heterogeneous Materials* (Springer, New York, 2002).
- [55] B. D. Hughes, *Random Walks and Random Environments* (Clarendon, Oxford, 1995).
- [56] P. C. Bressloff, V. M. Dwyer, and M. J. Kearney, *J. Phys. A* **29**, 6161 (1996).
- [57] N. G. Van Kampen, *Stochastic Processes in Physics and Chemistry* (North-Holland, Amsterdam, 1992).
- [58] H. C. Tuckwell, *Introduction to Theoretical Neurobiology* (Cambridge University Press, London, 1988), Vol. 2.
- [59] F. Santamaria, S. Wils, E. De Schutter, and G. J. Augustine, *Neuron* **52**, 635 (2006).